Polyphenol-rich *Trapa quadrispinosa* pericarp extract ameliorates high-fat diet induced non-alcoholic fatty liver disease by regulating lipid metabolism and insulin resistance in mice

Tunyu Jian[1], Han Lü[1*], Xiaoqin Ding[1], Yuexian Wu[1], Yuanyuan Zuo[1], Jiawei Li[1], Jian Chen[1,2*], Hong Gu[3]

[1] Institute of Botany, Jiangsu Province and Chinese Academy of Sciences, Nanjing, China
[2] Department of Food Science and Technology, College of Light Industry and Food Engineering, Nanjing Forestry University, Nanjing, China
[3] Department of Colorectal Surgery, Jiangyin Hospital of Traditional Chinese Medicine, Jiangyin, China

Corresponding Author:
Han Lü
No.1 Qianhuhoucun, Nanjing, Jiangsu, 210014, China
Email address: xiaohan1814@163.com
Jian Chen
No.1 Qianhuhoucun, Nanjing, Jiangsu, 210014, China
Email address: chenjian80@aliyun.com;

Abstract

In China, *Trapa quadrispinosa* (also called water caltrop) has long been used as a function food and folk medicine to treat diabetes mellitus for years. In the present study, the extract of *T. quadrispinosa* pericarp (TQPE) which mainly contains hydrolysable tannins was prepared to investigate the potential therapeutic action in non-alcoholic fatty liver disease (NAFLD) mice induced by high fat-diet (HFD). After the administration of TQPE (15, 30 mg/kg/day) for 8 weeks, the increased weight of body and liver were significantly suppressed. TQPE also ameliorated liver lipid deposition and reduced lipids parameters of blood in mice. Moreover, TQPE attenuated oxidative stress and showed a hepatoprotective effect in mice. TQPE was also found to decrease the value of homeostatic model assessment for insulin resistance. In addition, TQPE administration increased the phosphorylation of AMP-activated protein kinase (AMPK) and Acetyl-CoA carboxylase (ACC) and inhibited sterol regulatory element-binding protein (SREBP) in the liver tissue. Meanwhile, TQPE elevated insulin receptor substrate-1 (IRs-1) and protein kinase B (Akt) phosphorylation. These results reflected that, as a nature product, TQPE is

38 a potential agent for suppressing the process of NAFLD via regulation of the
39 AMPK/SREBP/ACC and IRs-1/Akt pathways.

40

Introduction

42 As a common chronic liver disease, Non-alcoholic fatty liver disease (NAFLD) is defined by
43 pathological accumulation of lipid in the liver without excess alcohol consumption (Golabi *et al.*
44 2017). Being a hepatic manifestation of metabolic syndrome, it is similar to those chronic
45 metabolic disorders, such as obesity, insulin resistance, type 2 diabetes mellitus (T2DM),
46 inflammation and cardiovascular disease (Bagherniya *et al.* 2018). NAFLD increases the risk of
47 progressive liver injury, which appears as a continuum disease progression, from simple steatosis
48 to liver failure and hepatocellular carcinoma (Suolang *et al.* 2019). NAFLD has emerged as a
49 worldwide serious public health burden, epidemiology of NAFLD have highlighted surprisingly
50 high prevalence in many countries (the estimated prevalence is 25-30% in adults) (Moore 2019;
51 Ratziu 2018). Therefore, there is a great demand for exploring effective therapeutic agents to
52 treat and prevent NAFLD.

53   The recent evidence indicated that fat accumulation and insulin resistance (IR) are intensely
54 associated with the development and progression of NAFLD (Araujo *et al.* 2018; Fan *et al.* 2018;
55 Jian *et al.* 2018). As a highly evolutionarily conserved sensor of cellular energy status, AMP-
56 activated protein kinase (AMPK) plays a critical role in regulating hepatic lipid metabolism
57 including lipolysis, glucose transport and gluconeogenesis (Brown & Goldstein 1997). Sterol
58 regulatory element-binding protein (SREBP), a key transcription factor in regulating liver lipid
59 synthesis, is the downstream of AMPK (Li *et al.* 2011). Acetyl-CoA carboxylase (ACC), a
60 member of lipogenic factor, is the downstream target of SREBP. AMPK activation
61 phosphorylates and inhibits ACC in adipose and hepatic tissues thus downregulate fatty acid
62 synthesis (Bijland *et al.* 2013; Zhang *et al.* 2018). In NAFLD model of many studies, it was
63 observed that the inhibition of phosphorylation of AMPK led to lipid accumulation by increasing
64 SREBP and inhibiting ACC phosphorylation (Chen *et al.* 2019; Li *et al.* 2018b; Park *et al.* 2019;
65 Zhou *et al.* 2017). Besides, IR is also strongly associated with hepatic lipid accumulation in
66 NAFLD. Insulin signaling transduction is dependent on insulin receptor substrate-1 (IRs-1), and
67 phosphorylation of IRs-1 give rise to insulin pathway activation (Fu *et al.* 2018; Saez-Lara *et al.*
68 2016). Moreover, for insulin signaling cascade conduction, Protein kinase B (Akt) is another
69 essential factor. Impairment of Akt activity has been demonstrated under NAFLD condition, thus
70 activated Akt (increased phosphorylation) could ameliorate hepatic steatosis and improve IR in
71 NAFLD model (Fan *et al.* 2018; Jung *et al.* 2018). Therefore, targeting regulation of AMPK and
72 insulin signaling pathway might be a new and useful therapeutic approach to drop lipid
73 accumulation and insulin resistance in NAFLD.

74   Nowadays, pharmacological studies have significantly expanded to screen natural products
75 for exploration of novel pharmaceutical agents. Many studies revealed that medicinal plant
76 extracts, herb formulas have remarkable therapeutic effect on NAFLD (Bagherniya *et al.* 2018;
77 Chen *et al.* 2017; Li *et al.* 2018a; Suolang *et al.* 2019). *Trapa quadrispinosa*, also called water

78 chestnut or water caltrop, is a floating-leaf aquatic plant, which is commonly cultivated in the
79 south of China, as well as in India and south east Asia. The fruit of water caltrop, is a function
80 food and folk medicine, which could be used to treat metabolic syndrome such as diabetes
81 mellitus (DM). But the pericarps of *T. quadrispinosa* were usually discarded in large quantities
82 after the seeds had been harvested. Interestingly, recent researches have demonstrated that the
83 pericarps of water caltrop also displayed multiple biological activities, including hypoglycemic
84 (Huang *et al*. 2016), anti-tumor (Lin *et al*. 2013), anti-inflammatory (Kim *et al*. 2015), anti-
85 oxidant effects and hepatprotective activity (Kim *et al*. 2014). To our knowledge, the therapeutic
86 effect of *Trapa quadrispinosa* pericarps extract (TQPE) in high-fat diet (HFD) induced NAFLD,
87 remains unknown.

88   The purpose of the present study was designed to determine whether *Trapa quadrispinosa*
89 pericarps extract (TQPE) could attenuate NAFLD induced by HFD in mice, also explore a
90 possible mechanism of this action.

91

Materials & Methods

93 **Chemicals and Reagents**
94 HPLC grade methanol used for the mobile phase in HPLC-DAD/QTOF analysis was obtained
95 from Tedia Co. Inc. (Fairfield, OH, USA). Formic acid in HPLC grade was taken from Acros
96 Organics (Geel, Belgium). Pure water was produced from a Milli-Q system (Millipore, Bedford,
97 MA, USA). Five standard compounds isolated from *T. quadrispinosa* were prepared and
98 identified according to our previous study (Lv *et al*. 2019). Gallic acid was obtained from
99 National Institutes for Food and Drug Control of China (Beijing, China). The other reagents were
100 obtained from Sinopharm Chemical Reagent Co. Ltd. (Shanghai, China). A kit from KeyGen
101 Biotechnology (Nanjing, China) was used for the protein extraction and BCA protein assay.
102 Besides, the kits for detecting blood glucose, high-density lipoprotein cholesterol (HDL-c), low-
103 density lipoprotein cholesterol (LDL-c), total cholesterol (TC), triglycerides (TG), aspartate
104 aminotransferase (AST), alanine aminotransferase (ALT), superoxide dismutase (SOD) and
105 malonaldehyde (MDA) were all obtained from Nanjing Jiancheng Bioengineering Institute
106 (Nanjing, China). Determination of insulin by enzyme-linked immunosorbent assay (ELISA)
107 commercially kits were purchased from Beyotime Institute of Biotechnology (Haimen, China).

108   The antibodies of AMPKα, p-AMPKα (Thr172), ACC, p-ACC, IRs-, p-IRs-1 (Tyr895),
109 Akt, p-Akt (Ser473) for western blotting (WB) were purchased from Cell Signaling Technology
110 (Danvers, MA, USA). SREBP was obtained from Santa Cruz Biotechnology (Santa Cruz, USA).
111 Anti-rabbit/anti-mouse IgG and HRP-linked antibody were purchased from Cell Signaling
112 Technology (Danvers, USA).

113 **Preparation and characterization of *Trapa quadrispinosa* pericarp extract (TQPE)**
114 The air-dried *T. quadrispinosa* (collected in Shandong Zaozhuang of China) pericarp powder
115 (10.0 kg) was extracted twice with fifty litres 80% (v/v) ethanol by soaking at room temperature
116 for 14 days. After concentrating in vacuum at 50 °C, the extract was suspended in distilled water
117 and then partitioned by petroleum ether, ethyl acetate and normal-butanol successively. The ethyl

118   acetate extract was first concentrated and then dissolved in water, and later applied to a column
119   packed with macroreticular resin XAD16 (The Dow Chemical Company). The column was
120   orderly eluted with a gradient of H_2O, 10%, 40%, 60% and 95% ethanol solution. The 40%
121   ethanol elution was collected, concentrated and dried and finally the TQPE (175g) was obtained.
122   According to previous reported method, the total phenolic content of TQPE was measured
123   by the Folin-Ciocalteu phenol reagent (Singleton & Rossi 1965). Briefly, 1.0 mg of TQPE
124   extract was solved in 1.0 ml of methanol was used as test solution. After incubation with Folin-
125   Ciocalteu phenol reagent, the test solution was added 20% sodium carbonate to develop a color
126   and its absorbance was measured at 755 nm. The final value was expressed as gallic acid
127   (standard) equivalent.
128   5.0 mg/ml of TQPE (dissolved in methanol) was injected in an Agilent 6530 accurate-mass
129   quadrupole time-of-flight system (Agilent Technologies, CA, USA) for the HPLC-QTOF/MS
130   analysis. Separation was conducted by an Agilent ZORBAX SB-C18 column (1.8 μm, 4.6 × 100
131   mm; Waldbronn, Germany). The mobile phase was composed of Methanol (A) and 0.1% formic
132   acid (B) under gradient conditions (0-50 min, 10-50%A; 50-65 min, 50-100% A) at 1 ml/min.
133   The QTOF-MS equipped with an electrospray ion source operated in the negative ion mode at 4
134   kV capillary voltage, 10 L/min drying gas and 350 °C gas temperature. Mass range of scanning
135   was 100-1000 m/z. MassHunter Qualitative Analysis software (Agilent Technologies, USA) was
136   used to perform measurement and analysis.
137   Furthermore, HPLC-DAD was performed by Dionex Ultimate 3000 HPLC system (Thermo
138   Fisher Scientific, USA) equipped with a diode array-UV detector at 210 nm. Nucleosil C18
139   column (4.6 mm × 150 mm, 3 μm, ThermoFisher Scientific, USA) was used for separation. The
140   mobile phase was composed of Acetonitrile (A) and 0.05% trifluoroacetic acid (B) under
141   gradient conditions as followed: 0-5 min, 5%A; 5-15 min, 5-10% A; 15-55min, 10-25% A; 55-
142   65min, 25-100% A, the flow rate of HPLC was 1 ml/min.

143   **Animals**
144   The male ICR mice were obtained from Shanghai Sino-British SIPPR/BK Lab Animal Co., Ltd.
145   (China) and they were maintained in controlled condition as our previous study described (Jian *et*
146   *al*. 2018).

147   **Experimental protocol**
148   At first stage, mice were provided either a normal chow diet (10% of calories) or a high fat diet
149   (60% of calories) for 4 weeks, which were obtained from Shanghai Lab-oratory Animal Co. Ltd.
150   (Shanghai, China). Then, the high fat diet-fed mice were randomly divided into 3 groups: one
151   control group and two test groups, the test groups were administered with low dose of TQPE (15
152   mg/kg) and high dose of TQPE (30 mg/kg) per day. Normal control groups (CON) and high fat
153   diet-fed mice control (HFD) group were treated with solution of 0.5% CMC-Na. All mice in
154   each group were administrated relevant reagents for another 8 weeks. In the end of experimental
155   period, all the mice were fasted for 12 h, then anesthetized and euthanized by isoflurane gas.
156   Thereafter, the serum was separated from blood and the liver was removed and weighted. All the
157   samples were stored at -80°C condition before use.

158 **Biochemical parameters analysis**
159 According to the commercial kits instructions, serum TC, HDL, LDL, TG, SOD, MDA, ALT
160 and AST concentrations were determined in a microplate reader (Molecular Device, CA, USA).
161 Serum insulin level was determined by using ELISA commercially kits. The HOMA-IR
162 (Homeostatic model assessment for insulin resistance) value which was calculated as fasting
163 blood glucose (mmol/L) × fasting serum insulin (mIU/L)/22.5, was represented insulin
164 sensitivity.
165 **Liver pathological examination**
166 Liver tissues were fixed overnight at 4 °C in 4% paraformaldehyde and embedded in paraffin.
167 Sections (4 μm) were prepared for hematoxylin & eosin (H&E) stain. The histological images
168 were observed and photographed under an optical microscope (Carl Zeiss, Germany).
169 **Western blot analysis of liver tissue**
170 The total protein from the liver tissues was extracted using a commercial kit. Proteins from the
171 liver supernatant were quantified by a BCA kit. 25 μg of total proteins was separated on 8-10%
172 SDS-PAGE gel then transferred onto a PVDF membrane from Millipore (MA, USA). The
173 membrane was blocked for 2 h in 5% nonfat milk powder solution at room temperature. Then the
174 membranes were incubated with primary antibody at 4°C overnight. At the second day, the
175 membranes were incubated with secondary antibody at room temperature for 1-1.5 h. The
176 Membrane-bound antibodies complexes were noticed by ECL detection (Santa Cruz
177 Biotechnology, CA, USA). Tanon 5200 image system (Tanon, Shanghai, China) was used to
178 examine the signal. β-actin was employed to demonstrate the standard proteins quantity. ImageJ
179 software (NIH) was applied to quantify the density of western blotting bands
180 **Statistical analysis**
181 All results were expressed as mean ± SE from 10 mice. All statistical analyses were done
182 through the GraphPad Prism Software(Version 7.02, CA, USA). One-way ANOVA with a post-
183 hoc test was used for the statistical significance evaluation. $P < 0.05$ was indicated statistical
184 significance.

185

Results

186
187 **Analysis of chemical constituents and content of TQPE by HPLC-QTOF/MS and HPLC-**
188 **DAD**
189 According to Folin-Ciocalteu phenol test, the most abundant compound in the TQPE was
190 polyphenolics (hydrolysable tannins), the content of which was accounting for 91.7 ± 2.1%
191 (gallic acid equivalents). To furtherly understand the potential bioactive components in TQPE, a
192 HPLC-QTOF/MS assay was carried out. The base peak chromatogram of TQPE was illustrated
193 in Figure 1A. Eight phenolic compounds (R_t = 9.45, 23.07, 24.15, 24.76, 30.72, 35.58, 36.52 and
194 47.65 min) were tentatively identified according to previous studies (Hatano *et al*. 1990; Huang
195 *et al*. 2016). Their structures were shown in Figure 1B. The predominated polyphenols in TPQE
196 was gallic acid and its derivatives, which included hydrolysable gallotannins and gallates. We
197 also used HPLC-DAD method to calculate the content of five polyphenols in TPQE, which was

198   showed in Table 1. Gallic acid (Compound 1), 1,2,3-tri-*O*-galloyl-*β*-D-glucopyranose
199   (Compound 2), 1,2,3-tetra-*O*-galloyl-4,6-*O*-hexahydroxydiphenoyl-*β*-D- glucopyranoside
200   (Compound 6), 1,2,3,6-tetra-*O*-galloyl-*β*-D-glucopyranose (Compound 7), 1,2,3,4,6-penta-*O*-
201   hexahydroxydiphenoyl-*β*-D-glucopyranoside (Compound 8) were accounted for 696.56 ±
202   4.61mg/g.

203 **Effect of TQPE on the body and liver weight of HFD mice**
204   As showed in Figure 2A and Figure 2B, compared with the normal group, body weight in HFD
205   group and their liver to body weight ratio rose obviously ($P < 0.001$). Administration of TQPE
206   (15 and 30 mg/kg) significantly inhibited HFD induced growth in body weight and liver to body
207   weight ratios ($P < 0.01$). Treatment with TQPE reversed the continuing weight gain in both body
208   and liver.

209 **Histopathological examination**
210   Normal control group livers showed glossy and resilient appearance. In contrast, as showed in
211   Figure 2C, the NAFLD mice livers were enlarged with yellow necrosis foci appearing. After the
212   livers were treated with TQPE, the liver appearance improved in a dose-dependent manner
213   (Figure 2C).
214   Figure 2D displayed liver histology photo sections. In the control group, liver tissues
215   showed normal liver lobular structure without fatty accumulation or inflammatory. In HFD
216   treated mice, liver sections revealed significantly higher damage of hepatic lobule structures
217   compared with normal mice, while lipid droplets were also spotted in liver cells. As displayed in
218   Figure 2D, after treating with TQPE in 15 and 30 mg/kg, hepatocyte swelling as well as
219   quantities and volumes of lipid droplet were all alleviated. Morphology of liver lobular structure
220   almost regained normal status, especially in the mice treated with 30 mg/kg TQPE.

221 **TQPE ameliorates Lipid Parameters in NAFLD mice**
222   Relevant lipids parameters were detected to evaluate the effects of TQPE on lipid metabolism in
223   NAFLD mice. TC, TG and LDL content were markedly elevated ($P < 0.001$; Figure 3A, B and
224   D) along with a decrease in HDL level (Figure 3C; $P < 0.05$) in NAFLD mice compared to the
225   normal group. In Figure 3A-C, the data showed that administration of TQPE (15 mg/kg)
226   significantly reduced TC, TG and elevated HDL compared with the HFD group ($P < 0.01$).
227   Furthermore, after treatment with a high dose of TQPE at 30 mg/kg, besides above effects, it
228   dramatically decreased LDL but increased HDL level (Figure 3A-D; $P < 0.001$).

229 **TQPE changes the oxidative stress balance and reduces liver injury in NAFLD mice**
230   As demonstrated in Figure 4A and B, HFD group mice showed less adequate SOD and surplus
231   level of MDA in the serum compared to the control group. This phenomenon implying an
232   increased oxidative stress and a decrease of antioxidant capacity in HFD-induced NAFLD mice.
233   Treatment with TQPE ameliorated this symptom by significantly raising SOD and reducing
234   MDA level ($P < 0.001$, Figure 4A and B). In Figure 4C and D, compared with normal mice, the
235   contents of ALT and AST were seen elevating in the NAFLD mice. Administration of TQPE (15
236   and 30 mg/kg) significantly reduced ALT and AST levels indicating the recovery from liver
237   damage induced by HFD-induced NAFLD mice ($P < 0.001$).

238 **Effects of TQPE on serum insulin and Homeostatic Model Assessment of Insulin**
239 **Resistance (HOMA-IR)**
240 Insulin concentration in serum and HOMA-IR value were calculated to evaluate the effect of
241 TQPE on insulin blood level and action.
242   In HFD mice, both the serum insulin concentration and HOMA-IR value were increased
243 significantly, which indicating that there was an insulin resistance in NAFLD mice ($P < 0.001$,
244 Figure 5). Both the value of serum insulin concentration and HOMA-IR were significantly
245 decreased after the treatment of TQPE (15 and 30 mg/kg) in comparison with the HFD mice (P
246 < 0.001, Figure 5A and 5B). The data indicated that TQPE suppressed HFD-induced IR in
247 NAFLD mice.
248 **TQPE changes pathways participated in lipid metabolism and insulin resistance**
249 For further investigate the mechanism of TQPE preventing NAFLD, we detected the change of
250 proteins expression including AMPK, SREBP, ACC, IRs-1 and Akt in the liver tissue, which
251 were involved in lipid metabolism and insulin resistance. In Figure 6A-C, the phosphorylation of
252 AMPK and ACC were decreased along with an increase in SREBP in HFD group in comparison
253 with control group ($P < 0.001$). Meanwhile, compared with control group, in HFD mice liver, it
254 showed a drop of IRs-1 and Akt phosphorylation ($P < 0.001$; Figure 6D and E). Treatment with
255 TQPE at a high dose of 30 mg/kg markedly recovered the phosphorylation level of AMPK, ACC
256 and inhibited the expression of SREBP in HFD-induced NAFLD mice ($P < 0.001$; Figure 6A-C).
257 Additionally, TQPE (15 and 30 mg/kg) administration kept the similar level of IRs-1 and Akt
258 phosphorylation than the detected in the control mice ($P < 0.01$; Figure 6D and E).

Discussion

260 The current study investigated the therapeutic effect of *Trapa quadrispinosa* pericarp extract
261 (TQPE), on lipid accumulation and insulin resistance in HFD-induced NAFLD, and worked out
262 the possible mechanism. We concluded that TQPE attenuated HFD-induced lipid accumulation
263 in the liver, probably was mediated by the AMPK activation and SREBP-mediated lipogenesis
264 inhibition. TQPE also improved IR in NAFLD possibly through upregulating the levels of p-IRs-
265 1 and p-Akt protein (Figure 7).
266   It is widely accepted and confirmed that hepatic steatosis is the earliest stage of NAFLD,
267 which is manifested as accumulation of lipid in the liver. In nutrient oversupply states, ectopic
268 lipid accumulation is closely related to hyperglycemia and hyperlipidemia. AMPK is a crucial
269 key and important metabolic sensor and regulator of lipid and glucose metabolism in diverse
270 tissues and cells (Cheng *et al*. 2016; Day *et al*. 2017). Activated AMPK promotes energy
271 production, meanwhile, and represses ATP-consuming processes, to maintain energy status
272 balance (Gonzales *et al*. 1992; Ruderman & Prentki 2004). Both SREBP and ACC are two
273 downstream effectors of AMPK. For instance, AMPK activation inhibits fatty acid synthesis via
274 a reduction in the transcriptional activation of SREBP, which is a key transcription factor during
275 *de novo* lipogenesis in the regulation of lipogenic genes including *acc1* in the liver (Ahmed &
276 Byrne 2007; Zhou *et al*. 2017). AMPK activation also could switch off fatty acid synthesis
277 through ACC phosphorylation in adipose and hepatic tissues (Bijland *et al*. 2013; Zhang *et al*.

278   2018). As described, AMPK activation might reduce hepatic lipid accumulation via lipogenesis
279   inhibition, indicating that AMPK is a potential therapeutic target for the treatment of hepatic
280   steatosis in NAFLD (Zhou *et al*. 2017). Recent studies showed that many compounds are able to
281   activate AMPK in animal and cellular models to improve lipid metabolism in NAFLD, by
282   inhibiting SREBP and increasing phosphorylates of ACC (Chen *et al*. 2019; Kang *et al*. 2019;
283   Park *et al*. 2019). In our study, we explored the lipid contents comprising TC, TG and LDL, the
284   concentration of which were significantly lowered after TQPE treatment, while the HDL level
285   was enhanced in HFD-induced NAFLD ($P < 0.01$; Figure 3). We also found that TQPE at dose
286   of 30 mg/kg/day could obviously activate the phosphorylation of AMPK and ACC, while inhibit
287   SREBP expression ($P < 0.001$; Figure 7A-C). These results demonstrated that AMPK axis is
288   associated with the protective effects of TQPE in lipid metabolism under NAFLD status.
289   Impaired responsiveness to insulin evokes insulin resistance in NAFLD, hence, the
290   improvement of insulin sensitivity is important for the treatment of NAFLD. Insulin receptor
291   substrate-1 (IRs-1) is a core factor in insulin signaling transduction. Research showed that
292   phosphorylation of IRs-1 at Ser accounts for IR, while phosphorylation of IRs-1 at Tyr is
293   required for responses of insulin stimulates (Bhattacharyya *et al*. 2015; Xiao *et al*. 2018) . In
294   metabolic disorders, such as NAFLD and T2DM, impaired IRs-1 level was observed, for
295   instance, lipid accumulation in the liver was closely associated with increased serine
296   phosphorylation of IRs-1 (Araujo *et al*. 2018; Dallak 2018; Dong *et al*. 2019). Restoration of
297   IRs-1 might be a beneficial treatment for curing NAFLD (Yang *et al*. 2018; Zhou *et al*. 2018).
298   Protein kinase B (Akt) as downstream of IRs-1, plays an essential role in insulin signaling
299   cascade. In response to upstream signal of IRs-1 on Tyr, activated Akt increases hepatic glucose
300   uptake, glycogen synthesis and decreases lipogenesis (Cignarelli *et al*. 2019; Geidl-Flueck &
301   Gerber 2017; Guo 2014). Moreover, hepatic Akt activation enhances the insulin sensitivity
302   (Cignarelli *et al*. 2019; Ke *et al*. 2015). Therefore, IRs-1/Akt is important for hepatic insulin
303   signaling, regulates this pathway might be beneficial for treating NAFLD. In the current work,
304   the level of insulin and HOMA-IR value increased significantly in HFD-induced NAFLD ($P <$
305   0.001; Figure 5). This mechanism supported by decreased hepatic phosphorylation of IRs-1 on
306   Tyr ($P < 0.001$; Figure 6D). In parallel, there was also a significant decline in phosphorylation of
307   Akt ($P < 0.001$; Figure 6E) in NAFLD mouse model. TQPE administration with different doses
308   (15 and 30 mg/kg/day) reversed the high level of insulin and HOMA-IR value compared with
309   NAFLD mice ($P < 0.001$; Figure 5). This effect might be associated with restore phosphorylation
310   of IRs-1 and Akt ($P < 0.05$; Figure 6D, E) by TQPE to improve IR in NAFLD model.
311   In addition, ALT and AST are two hepatic enzymes, which are well-known key
312   biochemical markers for detecting liver damage in NAFLD mode (Katsagoni *et al*. 2017). In our
313   study, HFD treatment induced increasing of ALT and AST, while the administration of TQPE
314   (15 and 30 mg/kg/day) could revise these parameters ($P < 0.001$; Figure 4C, D). In comparison
315   with a dose of 2000 mg/kg of *T*. natans pericarp extract displaying antihyperglycemic effect in
316   rats (Yasuda *et al*. 2014), and based on exploratory studies of 50-100 mg/kg doses, we found that
317   a lower dose of 30 mg/kg of TQPE, also exerted a therapeutic action on HFD-induced NAFLD

318   in mice, while no significant abnormal changes were found in the present study, so we stepped
319   down doses for this study to provide a good safety margin. According to USA Food and Drug
320   Administration's instruction (Food and Drug Administration. 2005), the dose of 30 mg/kg TQPE
321   used in human is approximately 200 mg/day, thus this dose is acceptable for patients compared
322   to other clinical trials used (250-960 mg/day) (Chen *et al*. 2016; Qiu *et al*. 2013; Ried *et al*.
323   2013).

Conclusions

325   The pericarps of *T. quadrispinosa* is a kind of agricultural waste, that are usually discarded
326   in large quantities after the seeds had been harvested. From economic aspect, the present study
327   helps to discover polyphenol-rich extraction from this waste with medicinal value. The present
328   study demonstrated that *Trapa quadrispinosa* pericarp extract (TQPE) administration
329   significantly improve the metabolic parameters including the insulin resistance in high-fat diet-
330   induced NAFLD mice. The protective mechanisms of TQPE may be attributed to regulate
331   AMPK/SREBP/ACC and IRs-1/Akt signal pathways, which are involved in lipid metabolism
332   and IR, respectively. TQPE treatment provides a novel therapeutic strategy to prevent HFD-
333   induced NAFLD, however, there were still some limitations in this study i) the amount of food
334   eaten was not directly measured, however, observation by caretakers showed that the animals
335   were feeding and the loss of weight was not simply related to decreased eating; ii) the active
336   entity in the extract which is absorbed and found in the plasma of the mice was not determined.
337   In further studies, we warranted to determine the bioavailability of the active entity, and evaluate
338   the mechanisms by which polyphenolic mediates AMPK/SREBP/ACC and IRs-1/Akt in HFD-
339   induced NAFLD.

340

Acknowledgements

342   The authors would like to thank Mr. Shirong Yang (Centre for instrumental analysis, College of
343   Forestry, Nanjing Forestry University, Nanjing, China) for his useful help in the compound
344   structure analysis.

345

347   **Funding**
348   This research was funded by the National Natural Science Foundation of China (No. 81703224;
349   No. 81773885; No. 31770366), Jiangsu Province Science and Technology Modern Agricultural
350   Plan (No. BE2016383). Jiangsu Province Independent Innovation in Agricultural science and
351   technology fund (CX(18)3042). And Natural Science Foundation of the Jiangsu Province
352   (BK20160603). The authors are also indebted to the supports from Jiangsu Scientific and
353   Technological Innovations Platform (Jiangsu Provincial Service Center for Antidiabetic Drug
354   Screening) and Jiangsu Key Laboratory for the Research and Utilization of Plant Resources (No.
355   JSPKLB201825; No. JSPKLB201833).

356 **Competing Interests**

357 The authors declare there are no competing interests.

358 **Author Contributions**

359 Formal analysis, T.Y.J. and X.Q.D.; Investigation, T.Y.J., H.L., X.Q.D and Y.X.W.;

360 Methodology, Y.Y.Z. and J.W.L.; Project administration, H.L. and J.C.; Resources, H.G.;

361 Writing - original draft, T.Y.J. and H.L.; Writing – review & editing, J.C..

362 **Animal Ethics**

363 The following information was supplied relating to ethical approvals (i.e., approving body and

364 any reference numbers):

365   All animal experiments for the study followed the Guide for the Care and Use of Laboratory

366 Animals was approved by the Animal Ethics Committee of China Pharmaceutical University

367 (certificate number: SYXK2016-0011, approval date: 27 January 2016 to 26 January 2021).

368

369 # References

370 Ahmed MH, and Byrne CD. 2007. Modulation of sterol regulatory element binding proteins
371   (SREBPs) as potential treatments for non-alcoholic fatty liver disease (NAFLD). *Drug*
372   *Discovery Today* 12:740-747.10.1016/j.drudis.2007.07.009
373 Araujo LCC, Feitosa KB, Murata GM, Furigo IC, Teixeira SA, Lucena CF, Ribeiro LM, Muscara
374   MN, Costa SKP, Donato J, Jr., Bordin S, Curi R, and Carvalho CRO. 2018. Uncaria
375   tomentosa improves insulin sensitivity and inflammation in experimental NAFLD.
376   *Scientific Reports* 8:11013.10.1038/s41598-018-29044-y
377 Bagherniya M, Nobili V, Blesso CN, and Sahebkar A. 2018. Medicinal plants and bioactive
378   natural compounds in the treatment of non-alcoholic fatty liver disease: A clinical review.
379   *Pharmacological Research* 130:213-240.10.1016/j.phrs.2017.12.020
380 Bhattacharyya S, Feferman L, and Tobacman JK. 2015. Carrageenan Inhibits Insulin Signaling
381   through GRB10-mediated Decrease in Tyr(P)-IRS1 and through Inflammation-induced
382   Increase in Ser(P)307-IRS1. *Journal of Biological Chemistry* 290:10764-
383   10774.10.1074/jbc.M114.630053
384 Bijland S, Mancini SJ, and Salt IP. 2013. Role of AMP-activated protein kinase in adipose tissue
385   metabolism and inflammation. *Clinical Science (London, England: 1979)* 124:491-
386   507.10.1042/CS20120536
387 Brown MS, and Goldstein JL. 1997. The SREBP pathway: regulation of cholesterol metabolism
388   by proteolysis of a membrane-bound transcription factor. *Cell* 89:331-340
389 Chen IJ, Liu CY, Chiu JP, and Hsu CH. 2016. Therapeutic effect of high-dose green tea extract
390   on weight reduction: A randomized, double-blind, placebo-controlled clinical trial. *Clinical*
391   *Nutrition* 35:592-599.10.1016/j.clnu.2015.05.003
392 Chen K, Chen X, Xue H, Zhang P, Fang W, Chen X, and Ling W. 2019. Coenzyme Q10
393   attenuates high-fat diet-induced non-alcoholic fatty liver disease through activation of the
394   AMPK pathway. *Food Funct* 10:814-823.10.1039/c8fo01236a
395 Chen Q, Wang T, Li J, Wang S, Qiu F, Yu H, Zhang Y, and Wang T. 2017. Effects of Natural
396   Products on Fructose-Induced Nonalcoholic Fatty Liver Disease (NAFLD). *Nutrients*
397   9.10.3390/nu9020096

398 Cheng S, So WY, Zhang D, Cheng Q, Boucher BJ, and Leung PS. 2016. Calcitriol Reduces
399   Hepatic Triglyceride Accumulation and Glucose Output Through
400   Ca2+/CaMKKβ/AMPK Activation Under Insulin-Resistant Conditions in Type 2
401   Diabetes Mellitus. *Current Molecular Medicine* 16:747-758
402 Cignarelli A, Genchi VA, Perrini S, Natalicchio A, Laviola L, and Giorgino F. 2019. Insulin and
403   Insulin Receptors in Adipose Tissue Development. *Int J Mol Sci*
404   20.10.3390/ijms20030759
405 Dallak MA. 2018. Acylated ghrelin induces but deacylated ghrelin prevents hepatic steatosis
406   and insulin resistance in lean rats: Effects on DAG/ PKC/JNK pathway. *Biomedicine and*
407   *Pharmacotherapy* 105:299-311.10.1016/j.biopha.2018.05.098
408 Day EA, Ford RJ, and Steinberg GR. 2017. AMPK as a Therapeutic Target for Treating
409   Metabolic Diseases. *Trends in Endocrinology and Metabolism* 28:545-
410   560.10.1016/j.tem.2017.05.004
411 Dong R, Yang X, Wang C, Liu K, Liu Z, Ma X, Sun H, Huo X, Fu T, and Meng Q. 2019.
412   Yangonin protects against non-alcoholic fatty liver disease through farnesoid X receptor.
413   *Phytomedicine* 53:134-142.10.1016/j.phymed.2018.09.006
414 Fan Y, He Z, Wang W, Li J, Hu A, Li L, Yan L, Li Z, and Yin Q. 2018. Tangganjian decoction
415   ameliorates type 2 diabetes mellitus and nonalcoholic fatty liver disease in rats by
416   activating the IRS/PI3K/AKT signaling pathway. *Biomedicine and Pharmacotherapy*
417   106:733-737.10.1016/j.biopha.2018.06.089
418 Food and Drug Administration. 2005. Guidance for industry: estimating the maximum safe
419   starting dose in initial clinical trials for therapeutics in adult healthy volunteers. *Center for*
420   *Drug Evaluation and Research (CDER).*7
421 Fu D, Cui H, and Zhang Y. 2018. Lack of ClC-2 Alleviates High Fat Diet-Induced Insulin
422   Resistance and Non-Alcoholic Fatty Liver Disease. *Cellular Physiology and Biochemistry*
423   45:2187-2198.10.1159/000488164
424 Geidl-Flueck B, and Gerber PA. 2017. Insights into the Hexose Liver Metabolism-Glucose
425   versus Fructose. *Nutrients* 9.10.3390/nu9091026
426 Golabi P, Bush H, and Younossi ZM. 2017. Treatment Strategies for Nonalcoholic Fatty Liver
427   Disease and Nonalcoholic Steatohepatitis. *Clinics in Liver Disease* 21:739-
428   753.10.1016/j.cld.2017.06.010
429 Gonzales GF, Garcia-Hjarles M, and Velasquez G. 1992. Hyperprolactinaemia and
430   hyperserotoninaemia: their relationship to seminal quality. *Andrologia* 24:95-100
431 Guo S. 2014. Insulin signaling, resistance, and the metabolic syndrome: insights from mouse
432   models into disease mechanisms. *Journal of Endocrinology* 220:T1-T23.10.1530/JOE-
433   13-0327
434 Hatano T, Okonogi A, Yazaki K, and Okuda T. 1990. Trapanins a and b, oligomeric
435   hydrolyzable tannins from trapa japonica flerov. *Chem Pharm Bull* 38:2707-
436   2711.10.1016/j.chemosphere.2016.04.049
437 Huang HC, Chao CL, Liaw CC, Hwang SY, Kuo YH, Chang TC, Chao CH, Chen CJ, and Kuo
438   YH. 2016. Hypoglycemic Constituents Isolated from Trapa natans L. Pericarps. *Journal*
439   *of Agricultural and Food Chemistry* 64:3794-3803.10.1021/acs.jafc.6b01208
440 Jian T, Ding X, Wu Y, Ren B, Li W, Lv H, and Chen J. 2018. Hepatoprotective Effect of Loquat
441   Leaf Flavonoids in PM2.5-Induced Non-Alcoholic Fatty Liver Disease via Regulation of
442   IRs-1/Akt and CYP2E1/JNK Pathways. *Int J Mol Sci* 19.10.3390/ijms19103005
443 Jung TW, Park HS, Choi GH, Kim D, and Lee T. 2018. beta-aminoisobutyric acid attenuates
444   LPS-induced inflammation and insulin resistance in adipocytes through AMPK-mediated
445   pathway. *Journal of Biomedical Science* 25:27.10.1186/s12929-018-0431-7
446 Kang MC, Ding Y, Kim HS, Jeon YJ, and Lee SH. 2019. Inhibition of Adipogenesis by
447   Diphlorethohydroxycarmalol (DPHC) through AMPK Activation in Adipocytes. *Marine*
448   *Drugs* 17.10.3390/md17010044

449 Katsagoni CN, Georgoulis M, Papatheodoridis GV, Panagiotakos DB, and Kontogianni MD.
450   2017. Effects of lifestyle interventions on clinical characteristics of patients with non-
451   alcoholic fatty liver disease: A meta-analysis. *Metabolism* 68:119-
452   132.10.1016/j.metabol.2016.12.006
453 Ke B, Zhao Z, Ye X, Gao Z, Manganiello V, Wu B, and Ye J. 2015. Inactivation of NF-kappaB
454   p65 (RelA) in Liver Improves Insulin Sensitivity and Inhibits cAMP/PKA Pathway.
455   *Diabetes* 64:3355-3362.10.2337/db15-0242
456 Kim B, Kim JE, Choi BK, and Kim HS. 2015. Anti-Inflammatory Effects of Water Chestnut
457   Extract on Cytokine Responses via Nuclear Factor-kappaB-signaling Pathway.
458   *Biomolecules & Therapeutics* 23:90-97.10.4062/biomolther.2014.080
459 Kim YS, Hwang JW, Han YK, Kwon HJ, Hong H, Kim EH, Moon SH, Jeon BT, and Park PJ.
460   2014. Antioxidant activity and protective effects of Trapa japonica pericarp extracts
461   against tert-butylhydroperoxide-induced oxidative damage in Chang cells. *Food and*
462   *Chemical Toxicology* 64:49-56.10.1016/j.fct.2013.11.018
463 Li Q, Li HJ, Xu T, Du H, Huan Gang CL, Fan G, and Zhang Y. 2018a. Natural Medicines Used
464   in the Traditional Tibetan Medical System for the Treatment of Liver Diseases. *Frontiers*
465   *in Pharmacology* 9:29.10.3389/fphar.2018.00029
466 Li Y, Xu S, Mihaylova MM, Zheng B, Hou X, Jiang B, Park O, Luo Z, Lefai E, Shyy JY, Gao B,
467   Wierzbicki M, Verbeuren TJ, Shaw RJ, Cohen RA, and Zang M. 2011. AMPK
468   phosphorylates and inhibits SREBP activity to attenuate hepatic steatosis and
469   atherosclerosis in diet-induced insulin-resistant mice. *Cell Metab* 13:376-
470   388.10.1016/j.cmet.2011.03.009
471 Li YC, Qiao JY, Wang BY, Bai M, Shen JD, and Cheng YX. 2018b. Paeoniflorin Ameliorates
472   Fructose-Induced Insulin Resistance and Hepatic Steatosis by Activating LKB1/AMPK
473   and AKT Pathways. *Nutrients* 10.10.3390/nu10081024
474 Lin Q, Shen J, Ning Y, Shen S, and Das UN. 2013. Inhibitory effects of water caltrop pericarps
475   on the growth of human gastric cancer cells in vitro. *Current Pharmaceutical Design*
476   19:7473-7478
477 Lv H, Jian T, and Ding X. 2019. Trapa natans pericarp extract ameliorates hyperglycemia and
478   hyperlipidemia in type 2 diabetic mice. *Revista Brasileira de*
479   *Farmacognosia*.10.1016/j.bjp.2019.04.011
480 Moore JB. 2019. From sugar to liver fat and public health: systems biology driven studies in
481   understanding non-alcoholic fatty liver disease pathogenesis. *Proceedings of the*
482   *Nutrition Society*:1-15.10.1017/S0029665119000570
483 Park M, Yoo JH, Lee YS, and Lee HJ. 2019. Lonicera caerulea Extract Attenuates Non-
484   Alcoholic Fatty Liver Disease in Free Fatty Acid-Induced HepG2 Hepatocytes and in
485   High Fat Diet-Fed Mice. *Nutrients* 11.10.3390/nu11030494
486 Qiu F, Jiang J, Ma Y, Wang G, Gao C, Zhang X, Zhang L, Liu S, He M, Zhu L, Ye Y, Li Q, and
487   Miao P. 2013. Opposite Effects of Single-Dose and Multidose Administration of the
488   Ethanol Extract of Danshen on CYP3A in Healthy Volunteers. *Evidence-Based*
489   *Complementary and Alternative Medicine* 2013:730734.10.1155/2013/730734
490 Ratziu V. 2018. The painful reality of end-stage liver disease in NASH. *Lancet Gastroenterol*
491   *Hepatol* 3:8-10.10.1016/S2468-1253(17)30365-5
492 Ried K, Frank OR, and Stocks NP. 2013. Aged garlic extract reduces blood pressure in
493   hypertensives: a dose-response trial. *European Journal of Clinical Nutrition* 67:64-
494   70.10.1038/ejcn.2012.178
495 Ruderman N, and Prentki M. 2004. AMP kinase and malonyl-CoA: targets for therapy of the
496   metabolic syndrome. *Nature Reviews: Drug Discovery* 3:340-351.10.1038/nrd1344
497 Saez-Lara MJ, Robles-Sanchez C, Ruiz-Ojeda FJ, Plaza-Diaz J, and Gil A. 2016. Effects of
498   Probiotics and Synbiotics on Obesity, Insulin Resistance Syndrome, Type 2 Diabetes

499   and Non-Alcoholic Fatty Liver Disease: A Review of Human Clinical Trials. *Int J Mol Sci*
500   17.10.3390/ijms17060928

501 Singleton V, and Rossi JN, M. H. 1965. Colorimetry of Total Phenolics with Phosphomolybdic-
502   Phosphotungstic Acid Reagents. *Am J Enol Viticult* 16:144-158.10.1186/s13063-017-
503   1796-8

504 Suolang PC, Liu BQ, Chen J, De J, Nima ZB, and Dunzhu CR. 2019. Protective effect and
505   mechanism of Qiwei Tiexie capsule on 3T3-L1 adipocytes cells and rats with
506   nonalcoholic fatty liver disease by regulating LXRalpha, PPARgamma, and NF-kappaB-
507   iNOS-NO signaling pathways. *Journal of Ethnopharmacology* 236:316-
508   325.10.1016/j.jep.2019.03.006

509 Xiao XH, Wang YD, Qi XY, Wang YY, Li JY, Li H, Zhang PY, Liao HL, Li MH, Liao ZZ, Yang J,
510   Xu CX, Wen GB, and Liu JH. 2018. Zinc alpha2 glycoprotein protects against obesity-
511   induced hepatic steatosis. *International Journal of Obesity (2005)* 42:1418-
512   1430.10.1038/s41366-018-0151-9

513 Yang Y, Wang J, Zhang Y, Li J, and Sun W. 2018. Black Sesame Seeds Ethanol Extract
514   Ameliorates Hepatic Lipid Accumulation, Oxidative Stress, and Insulin Resistance in
515   Fructose-Induced Nonalcoholic Fatty Liver Disease. *Journal of Agricultural and Food*
516   *Chemistry* 66:10458-10469.10.1021/acs.jafc.8b04210

517 Yasuda M, Yasutake K, Hino M, Ohwatari H, Ohmagari N, Takedomi K, Tanaka T, and Nonaka
518   G. 2014. Inhibitory effects of polyphenols from water chestnut (Trapa japonica) husk on
519   glycolytic enzymes and postprandial blood glucose elevation in mice. *Food Chemistry*
520   165:42-49.10.1016/j.foodchem.2014.05.083

521 Zhang D, Xie T, and Leung PS. 2018. Irisin Ameliorates Glucolipotoxicity-Associated beta-Cell
522   Dysfunction and Apoptosis via AMPK Signaling and Anti-Inflammatory Actions. *Cellular*
523   *Physiology and Biochemistry* 51:924-937.10.1159/000495395

524 Zhou B, Zhou DL, Wei XH, Zhong RY, Xu J, and Sun L. 2017. Astragaloside IV attenuates free
525   fatty acid-induced ER stress and lipid accumulation in hepatocytes via AMPK activation.
526   *Acta Pharmacologica Sinica* 38:998-1008.10.1038/aps.2016.175

527 Zhou Y, Ding YL, Zhang JL, Zhang P, Wang JQ, and Li ZH. 2018. Alpinetin improved high fat
528   diet-induced non-alcoholic fatty liver disease (NAFLD) through improving oxidative
529   stress, inflammatory response and lipid metabolism. *Biomedicine and Pharmacotherapy*
530   97:1397-1408.10.1016/j.biopha.2017.10.035

531

532

Concentration of five polyphenols in TPQE by HPLC-DAD analysis (n=3)

1 **Table 1.** Concentration of five polyphenols in TPQE by HPLC-DAD analysis (n=3)

Peak number	Compound name	Concentration (mg/g)
1	Gallic acid	27.66 ± 0.99
2	1,2,3-tri-*O*-galloyl-*β*-D-glucopyranose	19.89 ± 0.07
6	1,2,3-tetra-*O*-galloyl-4,6-*O*-hexahydroxydiphenoyl-*β*-D-glucopyranoside	182.12 ± 2.38
7	1,2,3,6-tetra-*O*-galloyl-*β*-D-glucopyranose	461.91±7.28
8	1,2,3,4,6-penta-*O*-hexahydroxydiphenoyl-*β*-D-glucopyranoside	4.04±0.09

Figure 1

Figures 1

The chromatogram of TQPE analyzed by HPLC-QTOF **(A)** and the structures of eight

dominated polyphenols in TQPE **(B-E)**

A

B

C

	R₁	R₂	R₃	R₄
2	G	G	H	H
3	H	H	H	G
4	H	G	H	H
5	G	H	H	G
6	G	G	(s)-HHDP	
7	G	G	H	G
8	G	G	G	G

D

E

G=

(S)-HHDP=
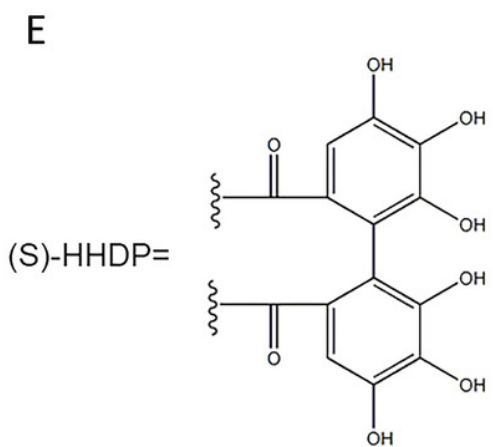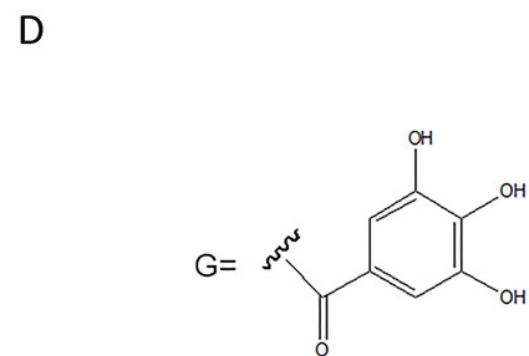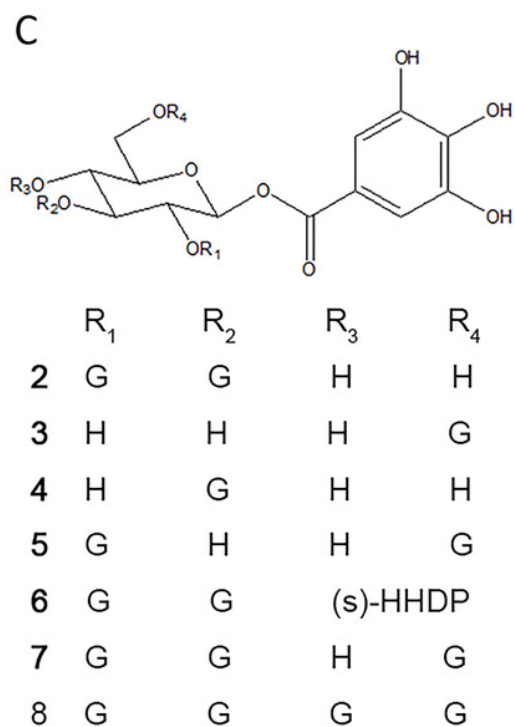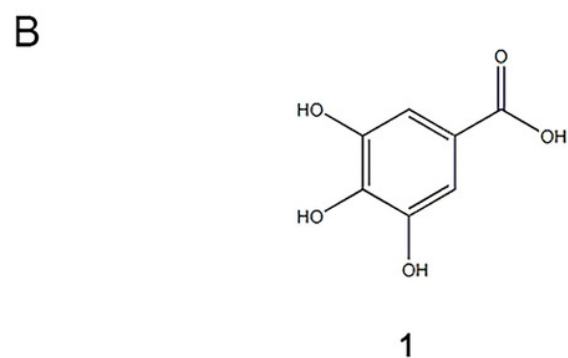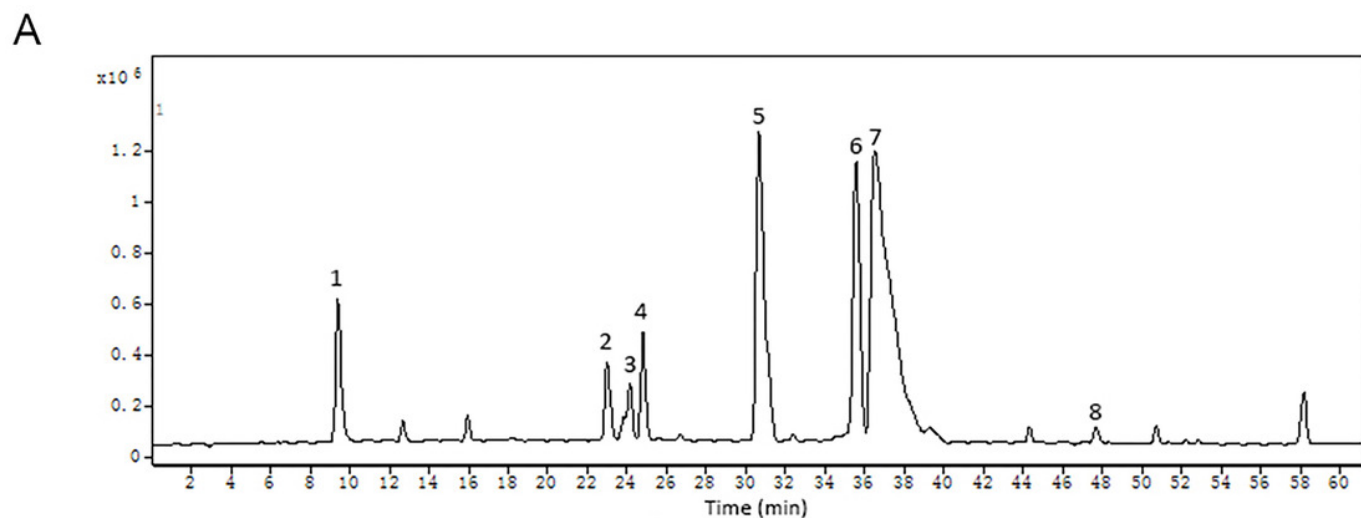
Figure 2

Figure 2

Body weight **(A)**, ratios of liver to body weight (%) **(B)**, appearance of the liver **(C-F)**, histological analysis of liver tissues (H&E, 200× magnification) **(G-J)**. All the results were presented as mean ± SE (n=10). $^{###}$ $P < 0.001$ vs. the CON group; ** $P < 0.01$, *** $P < 0.001$ vs. the HFD group.

A

B

C

CON

D

HFD

E

HFD+TQPE 15mg/kg

F

HFD+TQPE 30mg/kg

G

CON

H

HFD

I

HFD+TQPE 15mg/kg

J

HFD+TQPE 30mg/kg
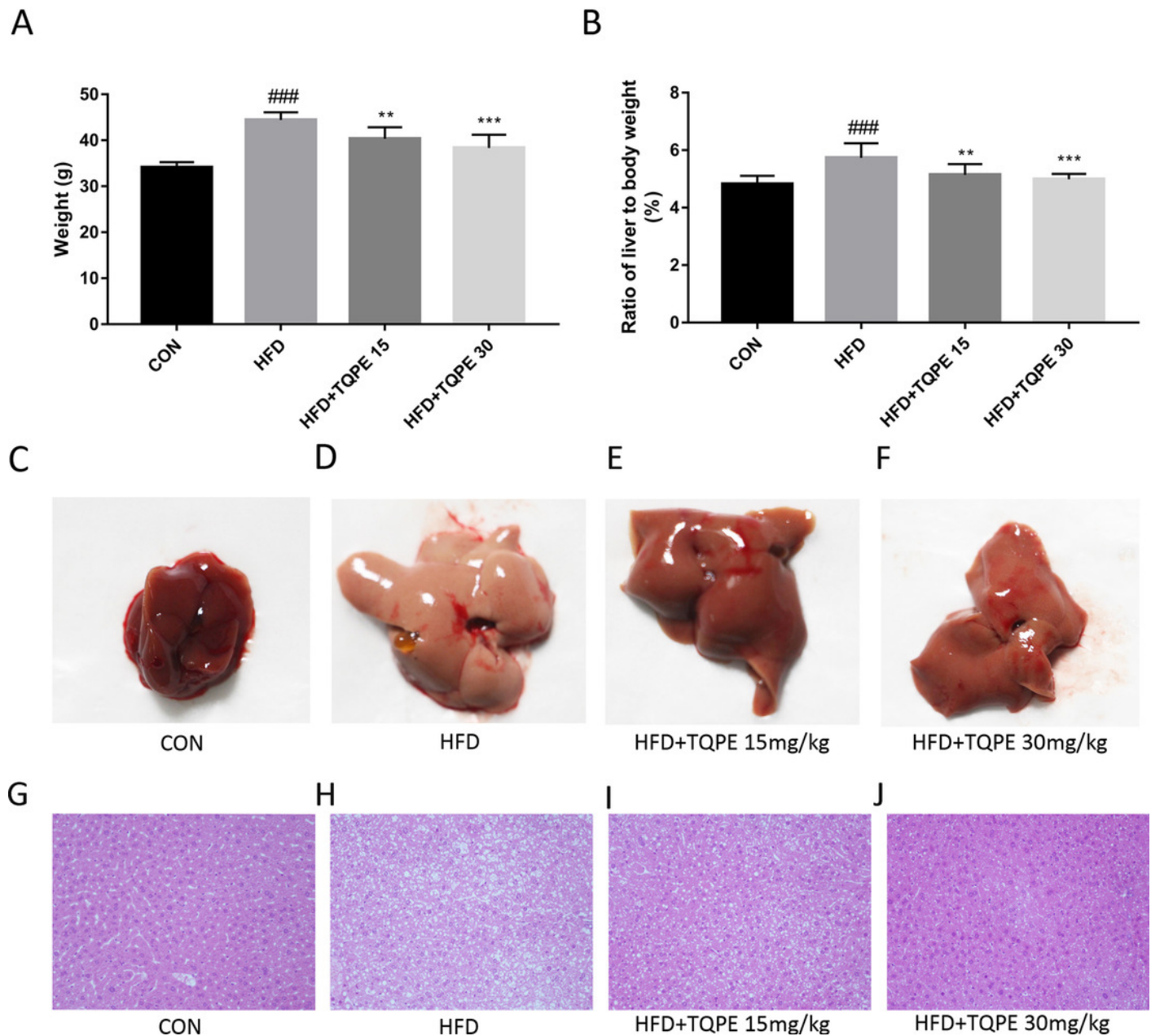
Figure 3

Figure 3

Effects of TQPE in HFD-induced NAFLD on plasma total cholesterol (TC) **(A)**, triglycerides (TG) **(B)**, high-density lipoprotein cholesterol (HDL) **(C)**, and low-density lipoprotein cholesterol (LDL) **(D)** were measured. All the results were presented as mean ± SE (n=10). $^{\#} P < 0.05$, $^{\#\#\#} P < 0.001$ vs. the CON group; $^{**} P < 0.01$, $^{***} P < 0.001$ vs. the HFD group.
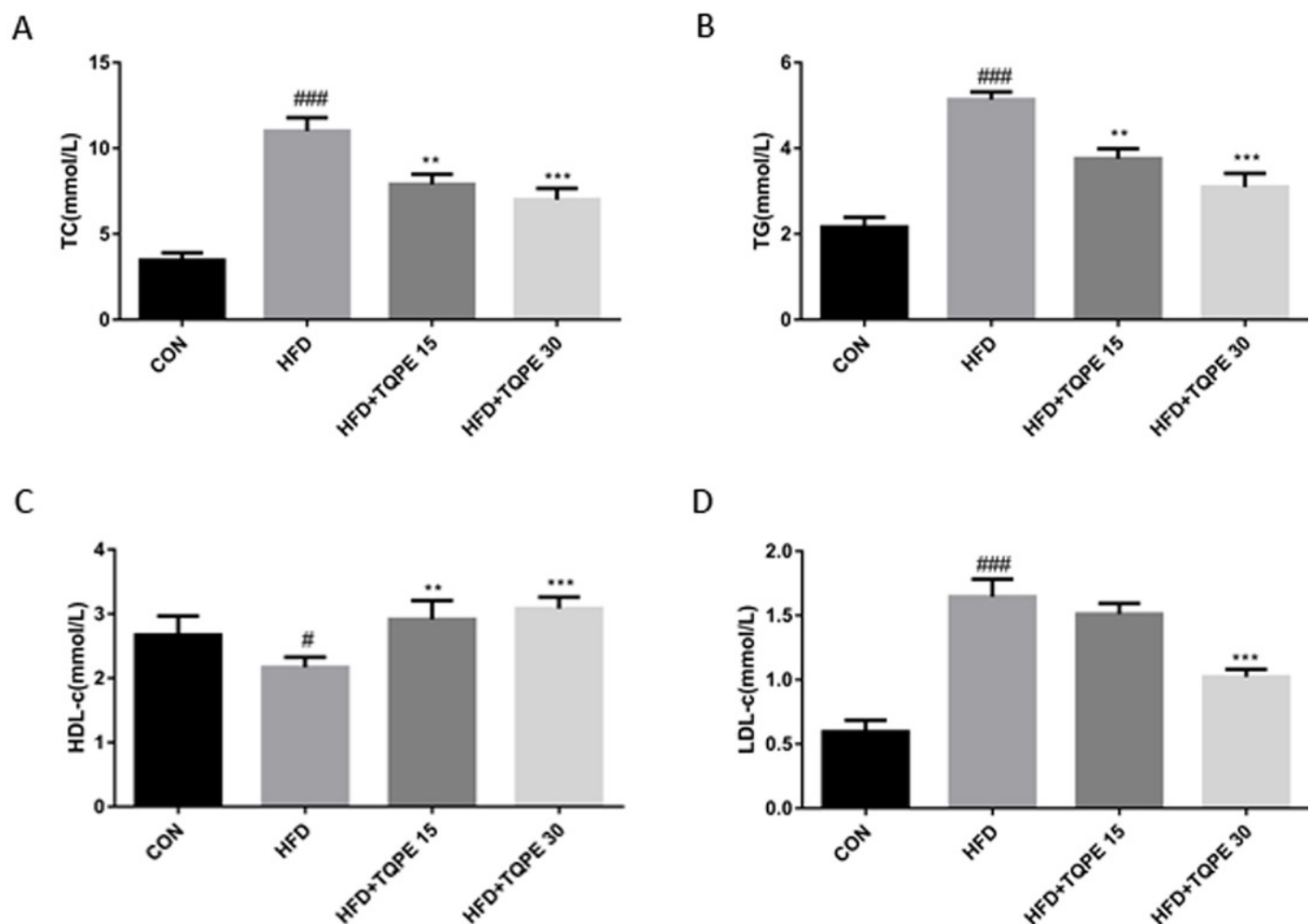
Figure 4

Figure 4

TQPE administration inhibits oxidative stress and liver injury in NAFLD. The levels of SOD **(A)**, MDA **(B)**, ALT **(C)** and AST **(D)** in the serum were measured. All the results were presented as mean ± SE (n=10). $^{###}$ *P* < 0.001 vs. the CON group; *** *P* < 0.001 vs. the HFD group.

A

B

C

D
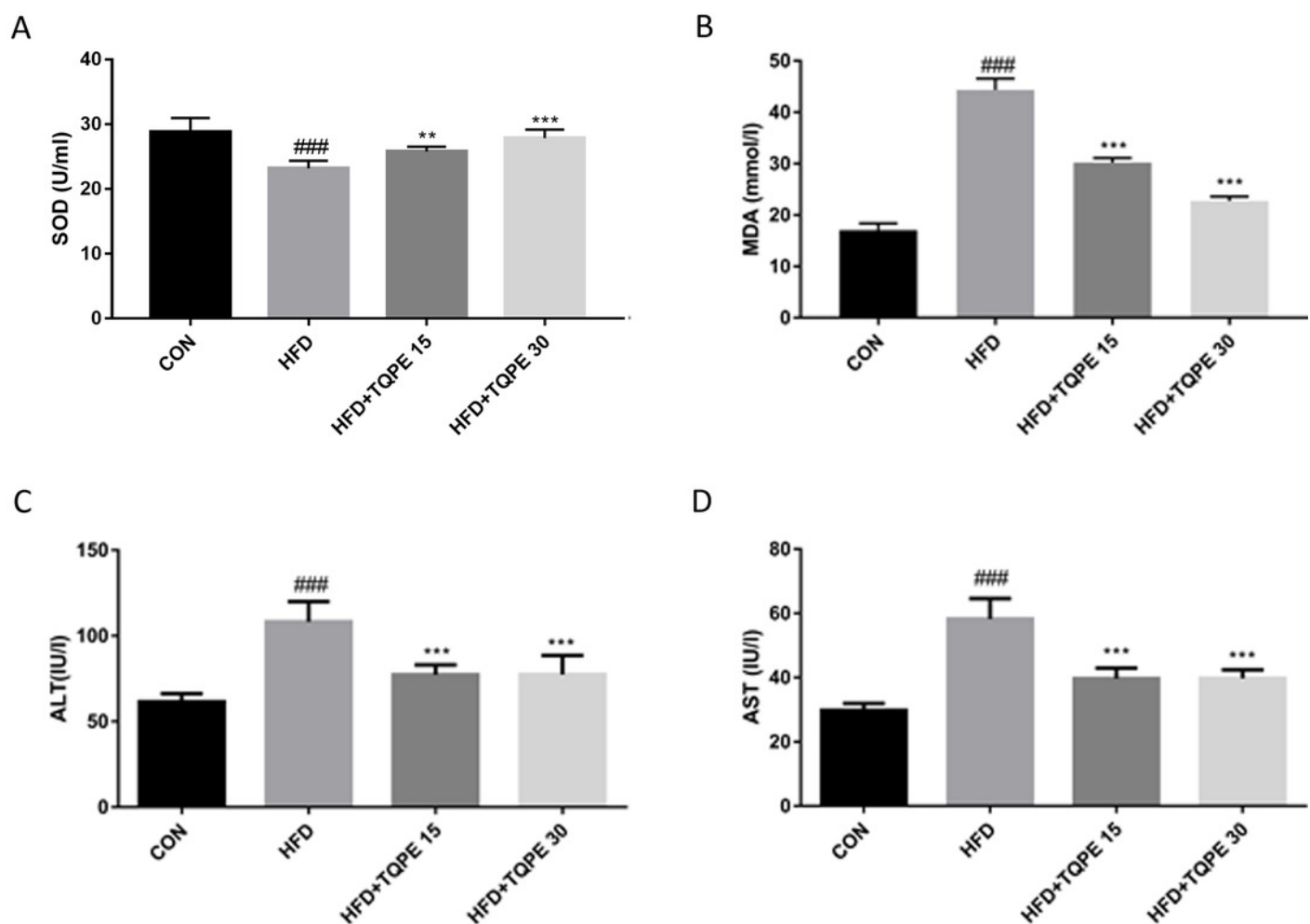
Figure 5

Figure 5

Effects of TQPE on insulin and HOMA-IR in HFD-induced NAFLD. The levels of insulin **(A)** in the serum and HOMA-IR value **(B)** were measured. All the results were presented as mean ± SE (n=10). [###] $P < 0.001$ vs. the CON group; [***] $P < 0.001$ vs. the HFD group.

A

B
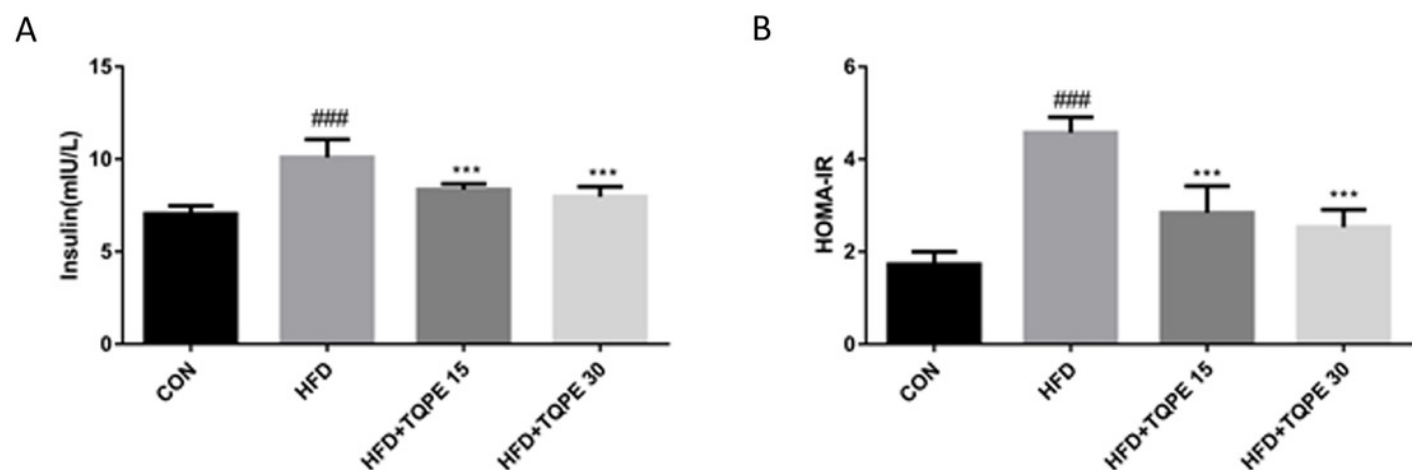
Figure 6

Figure 6

Effects of TQPE on AMPK, SREBP, ACC, IRs-1 and Akt in the liver tissue of HFD-induced NAFLD mice. p-AMPK, AMPK **(A-B)**, SREBP **(C-D)**, p-ACC, ACC **(E-F)**, p-IRs-1, IRs-1 **(G-H)**, p-Akt and Akt **(I-J)** expression were probed by western blotting. Results were presented as mean ± SE (n = 3). [###] $P < 0.001$ vs. the CON group; [*] $P < 0.05$, [**] $P < 0.01$, [***] $P < 0.001$ vs. the HFD group.
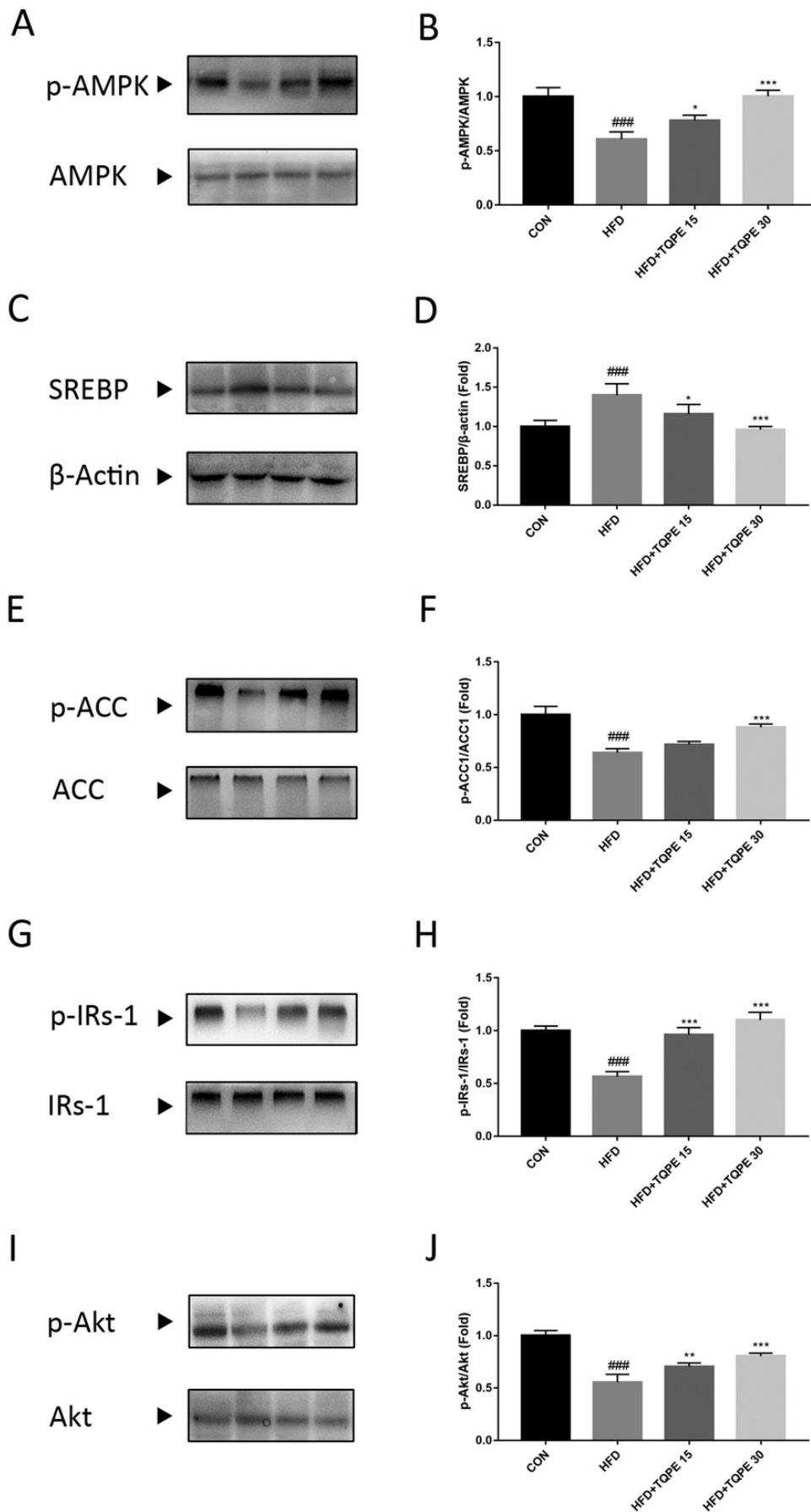
Figure 7

Figure 7

A schematic illustration of how TQPE interfered with lipid accumulation and IR in HFD-induced NAFLD mouse.